Prediction of ultimate strength of FRP-confined predamaged concrete using backward multiple regression motivated soft computing methods

I. A. Tijani[a], A. I. Lawal[b,c], N. O. Ogunsola[d], S. Kwon[b*]

[a]School of Engineering, The University of British Columbia, Kelowna, BC, V1V 1V7, Canada;
[b]Department of Energy Resources Engineering, Inha University Yong-Hyun Dong, Nam Ku, Incheon, Korea;
[c]Department of Mining Engineering, Federal University of Technology, Akure, Nigeria.
[d]Department of Mineral Resources and Energy Engineering, Jeonbuk National University, Jeonju-si, Jeollabuk-do, South Korea

*corresponding author: kwonsk@inha.ac.kr; ailawal@futa.edu.ng

Abstract

Confining structurally deficient concrete columns with externally bonded fiber-reinforced polymer (FRP) has been widely accepted as an effective technology for strengthening the ductility and strength of deficient concrete columns. However, prediction models for damaged and afterward repaired concrete based on soft computing methods are not available for the planning and maintenance of concrete structures. Therefore, this paper adopted two soft computing methods – artificial neural network (ANN) and Gaussian process regression (GPR) – to analyze observations obtained from 103 datasets of concentrically loaded FRP-confined predamaged concrete. The models only consider statistically significant variables with the ultimate strength of FRP-confined predamaged concrete. The statistically significant variables based on the multivariate regression analysis are corner radius ratio, FRP thickness, concrete strength, and damage degree. The coefficient of determination of the developed models is greater than 98% and there is a relatively low error between the measured and predicted values. The results of the current study highlight the merit of using soft computing methods in concrete technology given their extraordinary ability to comprehend multidimensional phenomena of concrete structures with ease and high predictivity over the existing empirical models.

Keywords: artificial neural network, concrete, damage degree, Gaussian process regression, soft computing methods, ultimate strength.

1. Introduction

Many concrete structures have reached the end of their design service life. Also, suddenly increased service loads, environmental action, and inappropriate maintenance have caused many concrete structures to gradually deteriorate. Hence, resulting in a substantial reduction in the load-carry capacity of the key structural components of the infrastructures and subsequently causing safety issues. Thus, rehabilitation and retrofitting of the concrete structures become inevitable. The application of fiber-reinforced polymer (FRP) has become a commonly accepted technology for retrofitting and strengthening structurally deficient concrete structures [1–7]. Extensive studies have culminated that confining concrete structures with FRP significantly improves the mechanical properties of concrete columns [6,8–16].

Generally, FRP-retrofitted structures – strengthened structures before damage – behaves much differently from FRP-repaired structures – strengthened structures after damage [5,17]. The most common approach for assessing the mechanical behavior of FRP-repaired concrete structures is through laboratory tests of FRP-confined predamaged concrete [6,11,17,18]. Nevertheless, studying the mechanical response of concrete in laboratories is time- and cost-intensive. Different factors affect the mechanical properties of concrete structures. Typically, the damage degree, sectional properties of the concrete structures, the concrete strength, and the FRP properties are the major factors affecting the mechanical properties of FRP-confined predamaged concrete.

The ability to forecast the peak strength of FRP-confined predamaged concrete is essential for proper planning and maintenance of the existing concrete structures. Typically, soft computing methods are proficient in solving an extensive range of multifaceted engineering problems. Currently, the application of soft computing methods in concrete technology is growing considerably, (e.g., [19–27]). To explore the advantages of these contemporaries in soft computing methods, two novel soft computing methods – artificial neural network (ANN) and Gaussian process regression (GPR) – have been used in this study to predict the ultimate strength of FRP-confined predamaged concrete. Hence, this paper aims at presenting data-driven techniques for FRP-confined predamaged concrete. Generally, these data-driven techniques were developed to reduce the time and associated cost of experimental setup for studying mechanical behaviour of concrete structures.

2. Overview of soft computing methods

2.1. Artificial neural network

Artificial neural networks (ANN) is one of the widely adopted soft computing methods which is established to model the human brain. The ability of ANN to match complex input parameters to output parameters, a streamlined approach with high performance, and a low computational rate, make this algorithm a popular technique [25]. Commonly, a multi-layer feedforward neural network is the most broadly adopted and simplest type of ANN and is capable of handling non-linear problems [28–31]. The main components of multi-layer feedforward neural network are the input layer, hidden layers, activation function, weights, an output layer, and neurons [19]. The input layer collects data from the external source and forwards it to the neurons in the hidden layers without processing it. The hidden layers perform the major computations, while the output layer presents the network calculations [32].

2.2. Gaussian process regression

Gaussian process regression (GPR) is another soft computing method that is a non-parametric Bayesian technique that captures an extensive diversity of relations between input and output parameters using a theoretical inestimable amount of functions and allows the data to determine the level of complexity through the Bayesian inference [33–35]. Typically, this technique expresses a reproductive process of the data that comprises hidden variables and stipulates the joint probability distribution of the hidden and observed random variables [35]. Unlike traditional regression techniques that use a technique of fitting several modes with a different quantity of clusters and then selecting a cluster using comparison metrics [36], this method fits a single model that can adapt its intricacy to the data.

3. Overview of FRP-confined predamaged concrete

Figure 1 illustrates the typical response curves of predamaged concrete, FRP-confined concrete, and, FRP-confined predamaged concrete. Here it is assumed that plain concrete is concentrically loaded to point C. After unplanned overloading, the concrete is completely unloaded to X, and then an FRP wrap is installed to strengthen the predamaged concrete. Typically, the concentrically loaded unconfined predamaged concrete and FRP-confined predamaged concrete will follow the load paths X-A-D and X-Z, respectively [6,18].

With reference to Fig.1; analytically, the damage degree of concrete is defined as the strength loss [37,38], as given in Eq. (1)

$$\delta = 1 - f_{cd} / f_{co} \quad (1)$$

where f_{co} and f_{cd} are the strengths of undamaged and unconfined predamaged concrete, and δ is the damage degree. A computational investigation based on soft computing methods previously unavailable is undertaken in this study to predict the ultimate strength of FRP-confined predamaged concrete. This study contributes to the repair and strengthening of damaged concrete under concentric loading using soft computing methods.

4. Overview of the test database

To predict the ultimate strength of FRP-confined predamaged concrete using soft computing methods, a database of concentrically loaded FRP-confined predamaged concrete was gathered from the literature. Inclusion of a test result into the database was based on the following requirements: (1) the concrete predamage was performed under concentric loading and repaired with carbon-FRP; (2) no inner steel reinforcement was present in the concrete; (3) the repair was performed using manual wet lay-up process of FRP wraps with the fibers oriented in the hoop direction of the column; and (4) the specimen was tested under concentric loading. The assembled database is presented in Table 1. The developed database compiled 103 data on FRP-confined predamaged concrete. The collected data on the ultimate strength of FRP-confined predamaged concrete covered 7 independent parameters: corner radius ratio ρ; FRP thickness t_f; concrete strength f_{co}; FRP elastic modulus E_f; damage degree δ; FRP rupture strain ε_f; and ultimate strength f_{cu}. More information about the test database can be referred to in the existing studies [11,18].

5. Model development

5.1 Backward multivariate regression

The adopted model datasets presented in Table 1 are subjected to backward multivariate regression (BMLR) to enable the identification of statistically significant variables. The backward multivariate regression implies that all the model variables participate in the regression models and are based on the statistical parameters – such as coefficient of correlation, coefficient of determination, Adj R-square, and p-values – which are used to access the parameters. The output of the analysis conducted using the OriginPro software is presented in Tables 2 to 4. Table 3 shows tha ANOVA of the model. The statistically significant variables are $2r/b$, f_{co}, δ,

and t_f (Table 4). Their p-values are far below 0.005. Therefore, the statistically significant parameters as presented in Table 4 were used in developing the proposed models.

Based on the results presented in Table 4, a regression equation – BMLR model – was formulated as given in Eq. (2). The performance of this regression equation is evaluated and presented under the results and discussion section.

$$f_{cu} = -36.3138 + 54.66411(2r/b) + 0.60366f_{co} - 0.41691\delta + 184.2782t_f \quad (2)$$

5.2. Normalization and performance metrics

The datasets in Table 1 have different units of measurement that can result in the overfitting of the soft computing methods. To eliminate, the effect of overfitting in the prediction models, existing models highlighted that datasets should be normalized [39–41]. Therefore, the datasets in Table 1 were normalized within the range of -1 and 1 for the ANN and 0 and 1 for the GPR model using Eq. (3). However, the same number of datasets were used in the training, testing, and validation of the proposed models.

$$x_{nm} = \frac{(n_{\max} - n_{\min})(x - x_{\min})}{(x_{\max} - x_{\min})} + n_{\min} \quad (3)$$

where x_{nm} is the normalized model parameter, x_{min} and x_{max} are the least and utmost values of the actual model parameter x, n_{min} and $n_{\max}$ are the smallest and highest values of the required normalization range. On the other hand, two performance indexes that are statistically sensitive to the deviation of prediction results from measured values are adopted to evaluate the models [42]. The indexes are mean squared error (MSE) and the coefficient of determination (R^2), – as given in Eqs (4) and (5) – respectively.

$$MSE = \frac{1}{m}\sum_{i=1}^{m}(y_{e_i} - y_{ex_i})^2 \quad (4)$$

$$R^2 = \left[\frac{\sum_{i=1}^{m}(y_{e_i} - \bar{y}_e)(y_{ex_i} - \bar{y}_{ex})}{\sqrt{\sum_{i=1}^{m}(y_{e_i} - \bar{y}_e)^2}\sqrt{\sum_{i=1}^{m}(y_{ex_i} - \bar{y}_{ex})^2}}\right]^2 \quad (5)$$

where y_e is the measured value, y_{ex} is the model predicted value, and m is the number of datasets.

5.3. ANN model

The normalized datasets were divided into training, testing, and validation datasets at the proportion of 70%, 15%, and 15% of the whole dataset, respectively in the MATLAB environment. The ANN was executed in the MATLAB environment. The feedforward backpropagation training algorithm was used with the Levenberg Marquardt training function. Typically, there is no fixed method to precisely determine the number of neurons in the hidden layers [28,29,32,39]. Therefore, 1-input, 1-hidden, and 1-output ANN architectures were tried with several trials of neurons in the hidden layer, and a hyperbolic tangent was defined as the transfer function for the hidden and output layers, respectively. The performance of the ANN architectures is presented in Fig. 2.

Based on the performance of the ANN architecture presented in Fig. 2, the selected optimum ANN is a 4-15-1 architecture as illustrated in Fig. 3. The weights and biases of the selected 4-15-1 architecture are presented in Table 5, while the performance of the selected architecture is shown in Fig. 4. Generally, it can be deduced that the error rate of the selected 4-15-1 architecture is low and that there is a high correlation between the measured and predicted results.

Generally, one of the drawbacks of an ANN model is that the relationship between the input variables and targeted output is usually not understood. This drawback can be solved by transforming the proposed ANN models into a mathematical expression that can be used for easy prediction of the targeted variable - ultimate strength of FRP-confined predamaged concrete - without the need to reconstruct a new ANN simulation [43–45]. Hence, the weights and biases of the 4-15-1 ANN architecture were extracted and presented in Table 5. Subsequently, the resulting mathematical expressions based on the weights and biases of the model are presented in Eqs. (6) and (7).

$$f_{cu} = 39.55\tanh\left(\sum_{i=1}^{15} x_i - 3.7853\right) + 81.55 \quad (6)$$

where x_i in Eq. (6) can be obtained from Table 5 as demonstrated in Eq. (7). It should however be noted that independent variables in the model (Eq. 7) are in the normalized form hence the data must be subjected to Eq. (3) before inserting them into Eq. (7).

$$\begin{cases} x_1 = 2.2828tanh(-0.01938\,(2r/b)\ -7.50709f_{co} - 4.6926\delta +\ 3.9958t_f - 5.0276) \\ x_2 = 1.37704\tanh(1.10647\,(2r/b)\ -4.1519f_{co} - 5.05247\delta +\ 0.34152t_f - 4.3304) \\ \quad\quad . \\ \quad\quad . \\ \quad\quad . \\ x_{14} = -4.0051\tanh(-2.1967\,(2r/b) + 1.4537f_{co} + 7.4786\delta - 0.3341t_f - 4.3954) \\ x_{15} = 2.44295\tanh(2.8501\,(2r/b) - 1.91109f_{co} - 1.0496\delta - 2.8828t_f + 0.8623) \end{cases} \quad (7)$$

5.4. GPR model

To develop the GPR model, the normalized datasets as adopted in the ANN model were used for training, testing, and validation purposes. Since GPR techniques are stochastic or probabilistic, the required mean, covariance, and likelihood functions were taken as constant, rational quadratic covariance, and Gaussian functions, respectively. The hyperparameters were first initialized and then optimized in conjunction with the intended training parameters. Thereafter the program was run to execute the training and the testing/validation of the GPR model. This program was implemented in the MATLAB environment. Therefore, LINiso (linear covariance function), LINard (linear covariance function with automatic relevance determination (ARD)), SEard (squared exponential covariance function with ARD), RQiso (isotropic rational quadratic covariance function), RQard (rational quadratic covariance function with ARD), and Materniso 1/2 covariance functions were tried. The performance of the different covariance functions is presented in Table 6. From Table 6, Materniso 1/2 covariance function performed better than the others and was selected for comparison with the proposed ANN and MLR models.

Based on the performance of the different covariance functions presented in Table 6, Materniso 1/2 is selected as the optimum covariance function for the GPR models. The performance of the selected covariance functions is shown in Fig. 5. Generally, it can be observed that the error rate of the selected covariance functions is low and there is a high correlation between the measured and predicted results. The performance of this model is evaluated and presented under the results and discussion.

6. Result and Discussion

6.1. Prediction models

Figures 6a and 6b present the comparison between the measured ultimate strength with the predicted ultimate strengths based on ANN and GPR models, respectively The linear least-square fit lines of the training and testing datasets with the ideal fit line are also presented in the

figures. The ±5% error bars are also included in the figures. The performances of the ANN model for the ultimate strength of FRP-confined predamaged concrete using the selected optimum 4-15-1 architecture network were assessed using the two performance indexes given in Eqs (3) and (4). Figure 6a illustrates the plots of the measured and predicted values for the training, testing, and validation datasets using the ANN model with 4-15-1 architecture. The linear least-square fit lines of the training and testing datasets with the ideal fit line are also presented in the figures. The ±5% error bars are also included in the figures. Similarly, the performance indexes were also used to evaluate the performances of the GPR model. Figure 6b illustrates the plots of the measured and predicted results for the training, testing, and validation datasets using the GPR model with Materniso 1/2 covariance functions. Also, the linear least-square fit lines of the training and testing datasets with the ideal fit line and the ±5% error bars are presented in the figures.

It can be observed that there is a good correlation between the measured values and the predicted values from the two soft computing methods. Generally, most of the data points are within the ±5% error bars. Hence, the error between the measured and predicted values is relatively low and the R^2 values are high. The results of the statistical indicators are summarized in Table 7.

As presented in Table 7, the R^2 values for the training, testing, and validation datasets of ANN model are 98.66%, 97.78%, and 98.96%, respectively. Similarly, the R^2 values for the training, testing, and validation datasets of GPR model are 99.39%, 99.76%, and 99.99%, respectively. On the other hand, the MSE values the training, testing, and validation datasets of ANN model are 4.9898, 6.0552, and 4.7290, respectively. Similarly, the MSE values the training, testing, and validation datasets of GPR model are 2.421, 1.2491, and 0.7444, respectively. Generally, the values of the performance indicators show that the proposed models can give prediction values that are close to the experimental values.

6.2. Evaluation of the ANN, GPR and BMLR models

The relationship between the measured values and the predicted results based on the 4-15-1 ANN architecture and Materniso 1/2 covariance GPR function are presented in Fig. 7 and Fig. 8, respectively. Furthermore, to examine the superiority of the models developed based on the soft

computing techniques, the relationship between the measured values and predicted results based on backward multivariate regression (Eq. 2) is also presented in Fig. 9.

It can be observed from Figs. 7 – 9 that the R^2 values of ANN, GPR, and BMLR models are 98.6%, 99.5%, and 85.99%, respectively. Meanwhile, as presented in Table 8, the computed MSE values between measured and predicted values based on ANN, GPR, and BMLR models are approximately 5.2, 2.0, and 51.7, respectively. The GPR model slightly outperformed the ANN model based on performance indexes while the BMLR model showed the least prediction performance. Although BMLR model was developed using statistically significant variables, the performance of the BMLR model has a least prediction performance as compared to the ANN and GPR models. Hence, it can be deduced that soft computing techniques aid the correlation between the measured data and predicted values.

7. Conclusion

This study used two soft computing methods – artificial neural network and Gaussian process regression – to developed models for the prediction of the ultimate strength of FRP-confined predamaged concrete. A test database of 103 datasets was assembled from the existing studies, the datasets comprise the strength of plain concrete, corner radius ratio, damage degree, the FRP elastic modulus, FRP thickness, FRP rupture strain, and the ultimate strength. The results of the current study illustrate the potential of using modern computing methods in predicting the ultimate strength of FRP-confined predamaged concrete. The following significant conclusions could also be drawn from the results of this study:

- Based on the multivariate regression analysis, the unconfined concrete strength, damage degree, corner radius, and thickness of the FRP materials are the major factors affecting the ultimate strength of FRP-confined predamage concrete.
- The mean squared error of the models based ANN, GPR, and backward multivariate regression analysis are approximately 5.1, 2.0, and 51.7, respectively. While, the R^2 values of ANN, GPR, and BMLR models are 98.6%, 99.5%, and 85.99%, respectively.
- The soft computing methods were able to predict the ultimate strength of FRP-confined predamaged concrete with sufficient accuracy and low error rates, as compared to the

performance of the model developed based on backward multivariate regression analysis only.

- Although both ANN and GPR models have almost the same prediction accuracy based on the statistical evaluation indexes, GPR slightly outperformed the ANN in the prediction of FRP-confined predamaged concrete.

The models established in this study applies to concentrically loaded FRP-confined predamaged concrete. Typically, the behaviour of concrete damaged by fire or other environmental effect prior to FRP repair could be signicantly differs from the mechanical response of concrete damaged by compression inflicted damage (as it in the assembled data in this study) before FRP repair. Also, the mechanical responses of FRP-confined predamaged concrete under eccentric and cyclic loading could be significantly different from the mechanical response of concrete structures under concrentric loading. Hence, future work is essential to advance the test database for FRP-confined predamaged concrete to consider the effect of more parameters such as damage caused by the environmental effect, attack by fire before repairing, inert filler, and fibers. Furthermore, the mechanical behavior of FRP-confined predamaged concrete under different types of loadings – e.g. eccentric and cyclic loading – could be substantially different from the behavior of concentrically loaded specimens. Hence, more study is required to examine the effect of different loadings on the FRP-confined predamaged concrete and to predict the mechanical behavior of FRP-confined predamaged concrete under different loadings using soft computing methods.

References

1. Dalgic, K.D., Ispir, M., and Ilki, A. "Cyclic and monotonic compression behavior of CFRP-jacketed damaged noncircular concrete prisms", *J. Compos. Constr*., **20**(1), p. 04015040 (2016).

2. Ma, G., Li, H., and Wang, J. "Experimental study of the seismic behavior of an earthquake-damaged reinforced concrete frame structure retrofitted with basalt fiber-reinforced polymer", *J. Compos. Constr*., **17**(6), p. 04013002 (2013).

3. Lim, J.C., and Ozbakkaloglu, T. "Lateral strain-to-axial strain relationship of confined

concrete". *J. Struct. Eng.*, **141**(5), p. 04014141 (2015).

4. Wu, Y.F., and Wei, Y.Y. "General stress-strain model for steel-and FRP-confined concrete", *J. Compos. Constr*., **19**(4), p. 04014069 (2015).

5. Tsonos, A.G. "Effectiveness of CFRP-jackets and RC-jackets in post-earthquake and pre-earthquake retrofitting of beam–column subassemblages". *Eng. Struct.*, **30**(3), pp. 777–93 (2008).

6. Tijani, I.A., Jiang, C., Lim, C.W., and Wu, Y.F. "Effect of load eccentricity on the mechanical response of FRP-confined predamaged concrete under compression". *J. Compos. Constr*., **24**(5), p. 04020057 (2020).

7. Tijani, I.A., Wu, Y.F., and Lim, C.W. "Effects of pre-damage on stress-strain relationship of partially confined concrete", *ACI Struct J*., **118**(1), pp. 61–72 (2020).

8. Ilki, A., Kumbasar, N., and Koc, V. "Low strength concrete members externally confined with FRP sheets", *Struct. Eng. Mech*., **18**(2), pp. 167–194 (2004).

9. Wei, Y.Y., and Wu, Y.F. "Unified stress-strain model of concrete for FRP-confined columns", *Constr. Build. Mater*., **26**(1), pp. 381–392 (2012).

10. Ilki, A., Peker, O., Karamuk, E., Demir, C., and Kumbasar, N. "FRP retrofit of low and medium strength circular and rectangular reinforced concrete columns", *J. Mater. Civ. Eng*., **20**(2), pp. 169–188 (2008).

11. Li, P., Sui, L., Xing, F., Li, M., Zhou, Y.W., and Wu, Y.F. "Stress–strain relation of FRP-confined predamaged concrete prisms with square sections of different corner radii subjected to monotonic axial compression", *J. Compos. Constr*., **23**(2), p. 04019001 (2019).

12. Ilki, A., Demir, C., Bedirhanoglu, I., and Kumbasar, N. "Seismic retrofit of brittle and low strength RC columns using fiber reinforced polymer and cementitious composites", *Adv. Struct. Eng*., **12**(3), pp. 325–347 (2009).

13. Ilki, A., and Kumbasar, N. "Behavior of damaged and undamaged concrete strengthened by carbon fiber composite sheets", *Struct. Eng. Mech*., **13**(1), pp. 75–90 (2002).

14. Wu, Y.F., and Jiang, C. "Quantification of bond-slip relationship for externally bonded

FRP-to-concrete joints", *J. Compos. Constr*., **17**(5), pp. 673–686 (2013).

15. Tijani, I.A., Wu, Y.F., and Lim, C.W. "Aggregate size effects and general static loading response on mechanical behavior of passively confined concrete", *Constr. Build. Mater*., **205**, pp. 61–72 (2019).

16. Tijani, I.A., Jiang, C., Lim, C.W., and Wu, Y.-F. "Eccentrically Loaded Concrete under Nonuniform Passive Confinement", *J. Struct. Eng*., **148**(1), p. 04021247 (2022).

17. Tijani, I.A., Wu, Y.F., and Lim, C.W. "Energy balance method for modeling ultimate strain of fiber-reinforced polymer-repaired concrete", *Struct Concr*., **21**(2), pp. 804–820 (2020).

18. Wu, Y.F., Yun, Y., Wei, Y.Y., and Zhou, Y.W. "Effect of predamage on the stress-strain relationship of confined concrete under monotonic loading", *J. Struct. Eng*., **140**(12), p. 04014093 (2014).

19. Ghanbari, S., Shahmansouri, A.A., Bengar, H.A., and Jafari, A. "Compressive strength prediction of high-strength oil palm shell lightweight aggregate concrete using machine learning methods", *Environ. Sci. Pollut. Res. Int.*, **30**, pp. 1096–1115 (2022).

20. Ashrafian, A., Shahmansouri, A.A., Akbarzadeh Bengar, H., and Behnood, A. "Post-fire behavior evaluation of concrete mixtures containing natural zeolite using a novel metaheuristic-based machine learning method", *Arch. Civ. Mech. Eng*., **22**(2), pp. 1–25 (2022).

21. Shahmansouri, A.A., Bengar, H.A, and Jafari, A. "Modeling the lateral behavior of concrete rocking walls using multi-objective neural network". *J. Concr. Struct. Mater*., **5**(2), pp. 110–128 (2020).

22. Shahmansouri, A.A., Yazdani, M., Hosseini, M., Bengar, H.A., and Ghatte, H.F. "The prediction analysis of compressive strength and electrical resistivity of environmentally friendly concrete incorporating natural zeolite using artificial neural network". *Constr. Build. Mater*., **317**, p. 125876 (2022).

23. Tijani, I.A., Lawal, A.I., and Kwon, S. "Machine learning techniques for prediction of ultimate strain of FRP-confined concrete", *Struct. Eng. Mech. An Int'l. J*., **84**(1), pp. 101–111 (2022).

24. Algaifi, H.A., Alqarni, A.S., Alyousef, R., Bakar, S.A., Ibrahim, M.H.W., Shahidan S., et al. "Mathematical prediction of the compressive strength of bacterial concrete using gene expression programming", *Ain Shams Eng J*., **12**(4), pp. 3629-3639 (2021).

25. Shahmansouri, A.A., Yazdani, M., Ghanbari, S., Akbarzadeh Bengar, H., Jafari, A., and Farrokh Ghatte, H. "Artificial neural network model to predict the compressive strength of eco-friendly geopolymer concrete incorporating silica fume and natural zeolite", *J. Clean Prod*., **279**, p. 123697 (2021).

26. Armaghani D.J., and Asteris P.G. "A comparative study of ANN and ANFIS models for the prediction of cement-based mortar materials compressive strength", *Neural Comput. Appl*., **33**(9), pp. 4501–4532 (2021).

27. Dao, D.V., Ly, H.B., Vu, H.L.T., Le, T.T., and Pham, B.T. "Investigation and optimization of the C-ANN structure in predicting the compressive strength of foamed concrete", *Mater*., **13**(5), p. 1072 (2020).

28. Lawal, A.I. "An artificial neural network-based mathematical model for the prediction of blast-induced ground vibration in granite quarries in Ibadan, Oyo State, Nigeria", *Sci. African*, **8**, p. e00413 (2020).

29. Lawal, A.I., and Kwon, S. "Application of artificial intelligence in rock mechanics: An overview". *J. Rock Mech. Geotech. Eng*., **13**, 248–266 (2021).

30. Fine, T.L., *Feedforward Neural Network Methodology*, Springer, New York, NY (1999).

31. Lawal, A.I., Aladejare, A.E., Onifade, M., Bada, S., and Idris, M.A. "Predictions of elemental composition of coal and biomass from their proximate analyses using ANFIS, ANN and MLR", *Int. J. Coal Sci. Technol*., 8(1), pp. 124–140 (2021).

32. Alpaydin, E., *Introduction to Machine Learning*, Third Edit., MIT Press (2014).

33. Schulz, E., Speekenbrink, M., and Krause, A. "A tutorial on Gaussian process regression: Modelling, exploring, and exploiting functions", *J. Math. Psychol*., **85**, pp. 1–16 (2018).

34. Williams, C.K.I. "Prediction with Gaussian processes: From linear regression to linear prediction and beyond", *In: Jordan, M.I. (eds) Learning in Graphical Models*, **89**, pp. 588–621 (1998).

35. Gershman, S.J., and Blei, D.M. "A tutorial on Bayesian nonparametric models", *J. Math. Psychol*., **56**(1), pp. 1–12 (2012).

36. Claeskens, G., and Hjort, N.L. *Model Selection and Model Averaging. Model Selection and Model Averaging*, Camb. Uni. Press (2001).

37. Chan, Y.N., Peng, G.F., and Anson, M. "Residual strength and pore structure of high-strength concrete and normal strength concrete after exposure to high temperatures", *Cem. Concr. Compos*., **21**(1), pp. 23–27 (1999).

38. Kumar, S., and Rao, C.K. "Strength loss in concrete due to varying sulfate exposures", *Cem. Concr. Res*., 25(1), pp. 57–62 (1995).

39. Lawal, A.I., and Idris, M.A. "An artificial neural network-based mathematical model for the prediction of blast-induced ground vibrations", *Int. J. Environ. Stud.*, **77**(2), pp. 318–334 (2020).

40. Said, K.O., Onifade, M., Lawal, A.I., and Githiria, J.M. "An artificial intelligence-based model for the prediction of spontaneous combustion liability of coal based on its proximate analysis", *Combust. Sci. Technol*., **193**(13), pp. 2350-2367 (2020).

41. Lawal, A.I., Kwon, S., Hammed, O.S., and Idris, M.A. "Blast-induced ground vibration prediction in granite quarries: An application of gene expression programming, ANFIS, and sine cosine algorithm optimized ANN", *Int. J. Min. Sci. Technol*., **31**(2), pp. 265–277 (2021).

42. Tijani I.A., and Zayed, T. "Gene expression programming based mathematical modeling for leak detection of water distribution networks", *Meas*., **188**, p. 110611 (2022).

43. Lawal, A.I., Oniyide, G.O., Kwon, S., Onifade, M., Köken, E., and Ogunsola, N.O. "Prediction of mechanical properties of coal from non-destructive properties: A comparative application of MARS, ANN, and GA", *Nat Resour Res*., **30**(6), pp. 4547–4563 (2021).

44. Lawal, A.I., Olajuyi, S.I., Kwon, S., and Onifade, M. "A comparative application of the Buckingham π (pi) theorem, white-box ANN, gene expression programming, and multilinear regression approaches for blast-induced ground vibration prediction", *Arab. J. Geosci.*, **14**(12), p. 1073 (2021).

45. Adesanya, E., Aladejare, A., Adediran, A., Lawal, A., and Illikainen, M. "Predicting shrinkage of alkali-activated blast furnace-fly ash mortars using artificial neural network (ANN)", *Cem. Concr. Compos*. 2021, **124**, p. 104265 (2021).

List of Figures

List of Tables

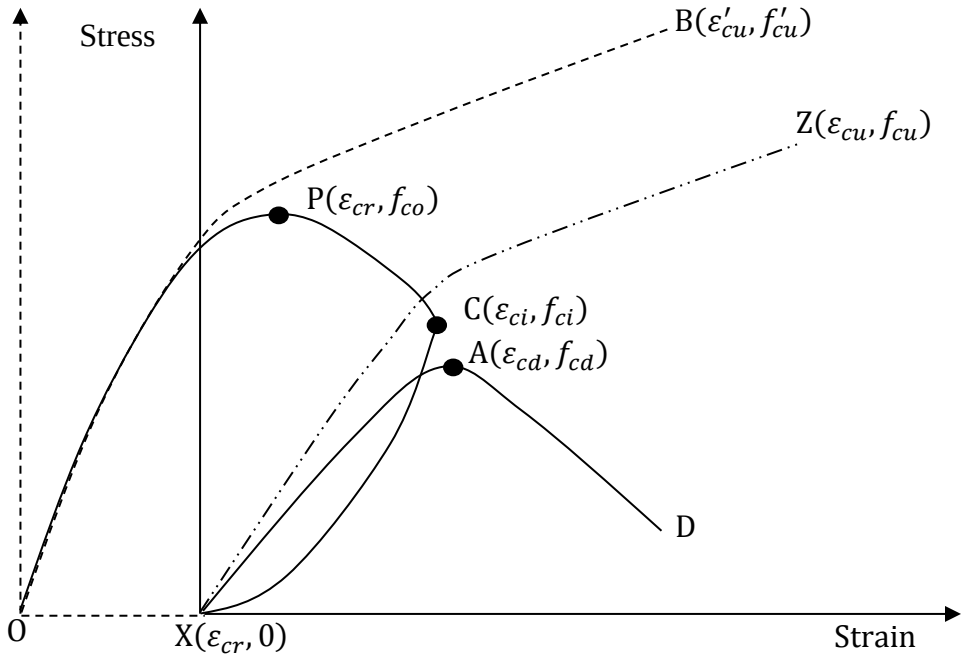

Fig. 3. Typical stress-strain curves

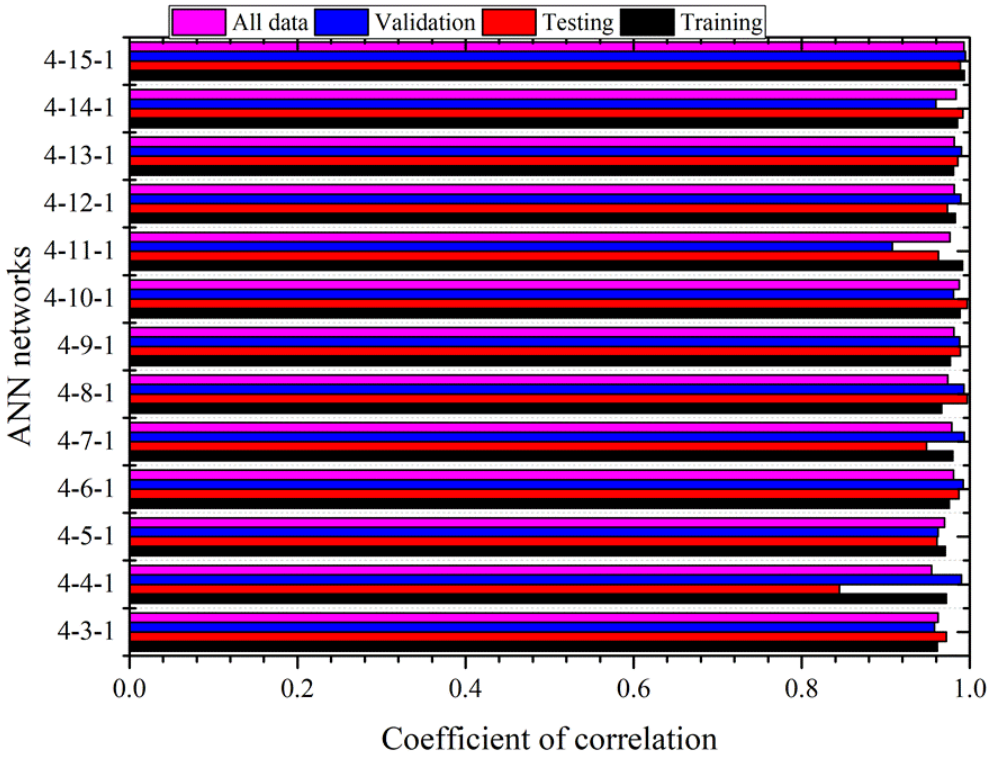

Fig. 4. Performance of different ANN architecture

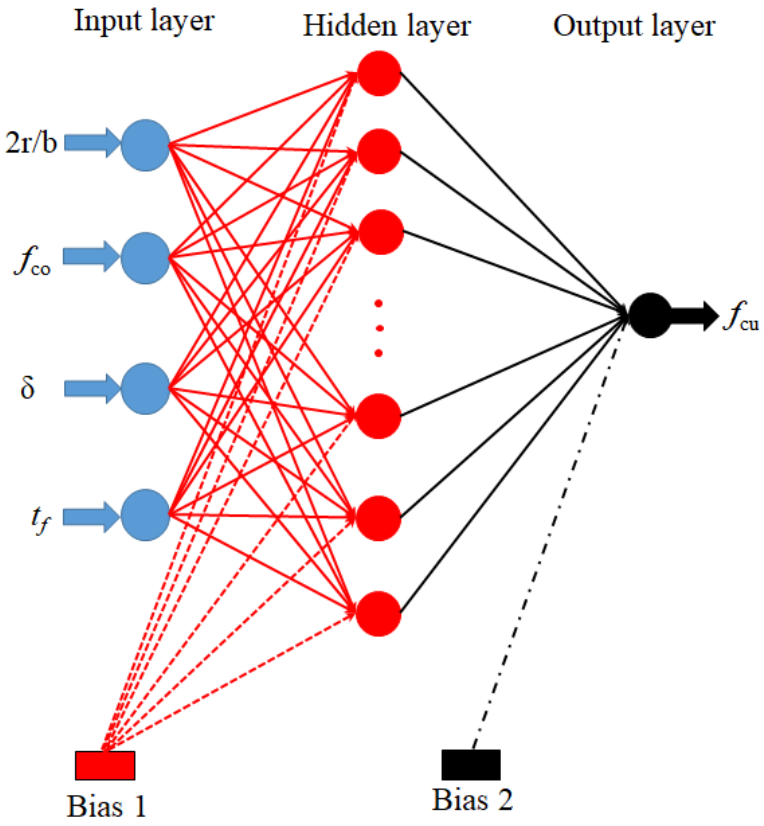

Fig. 5. Selected optimum ANN architecture

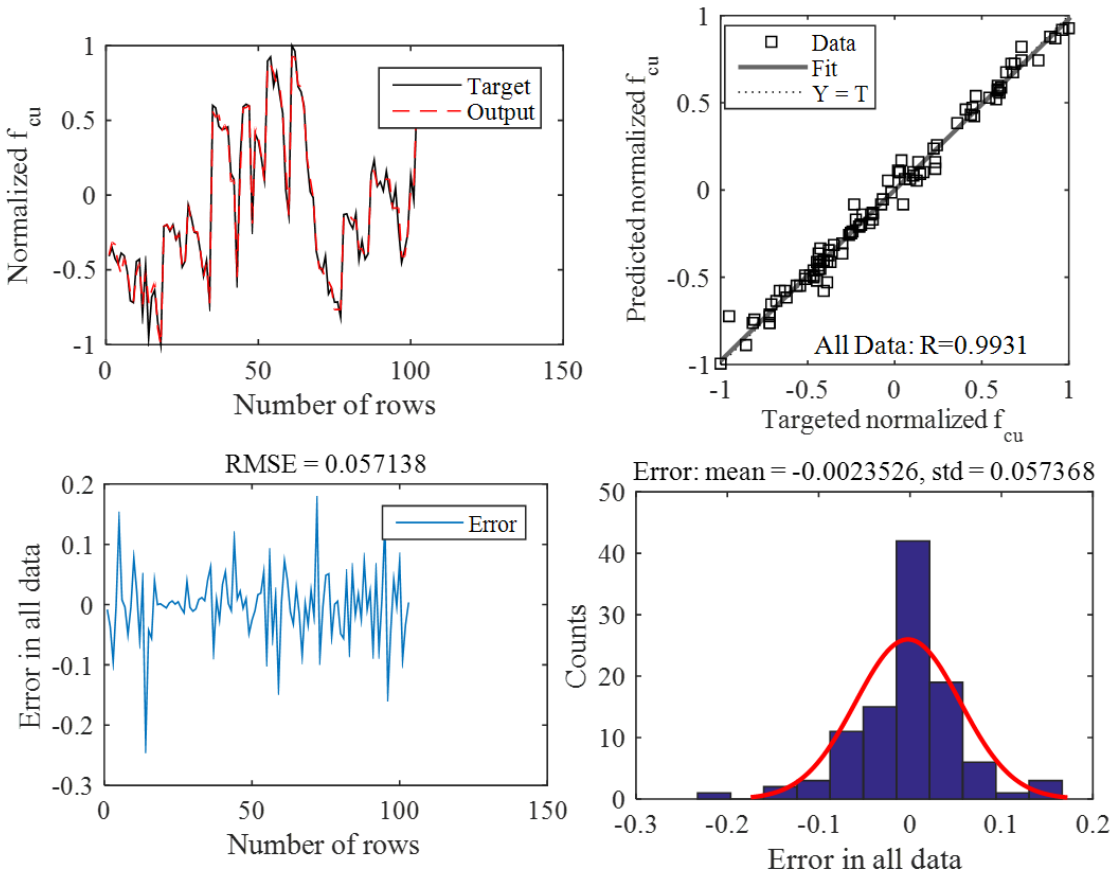

Fig. 6. The performance of the selected 4-15-1 architecture

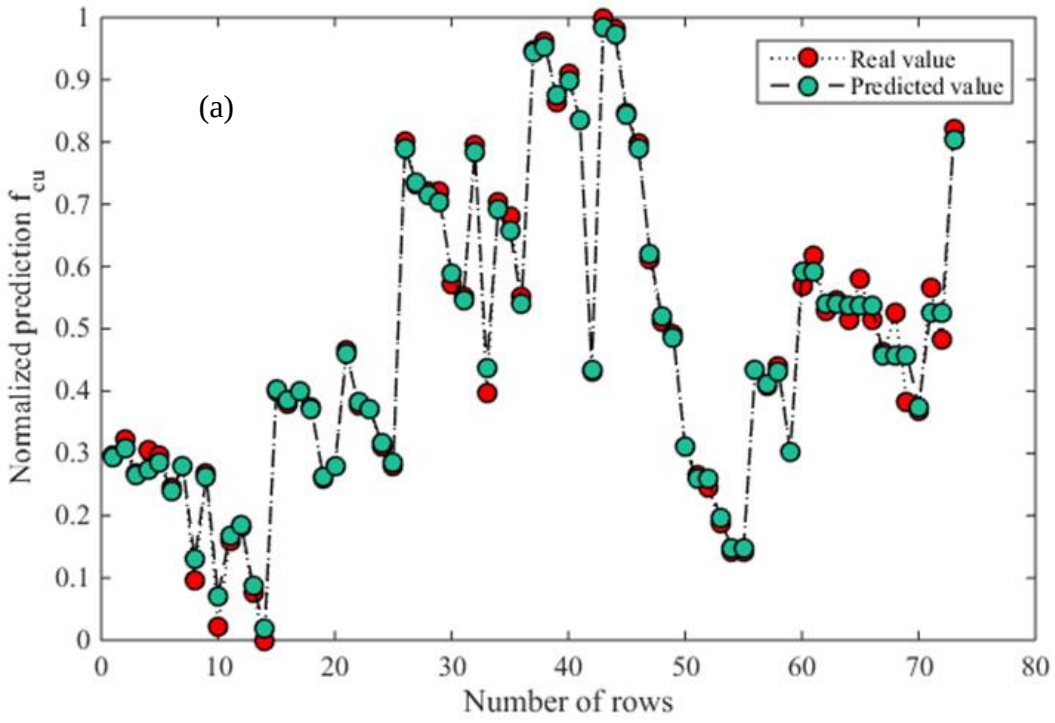

(a) actual and predicted values

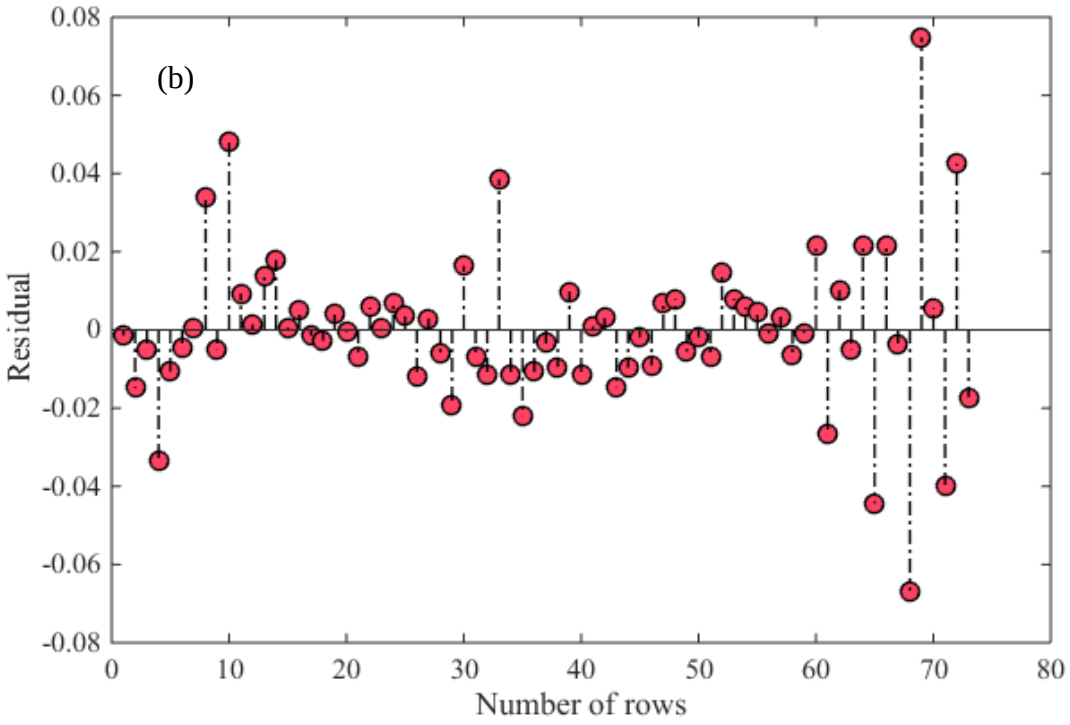

(b) residual

Fig. 7. The performance of Materniso 1/2 covariance functions

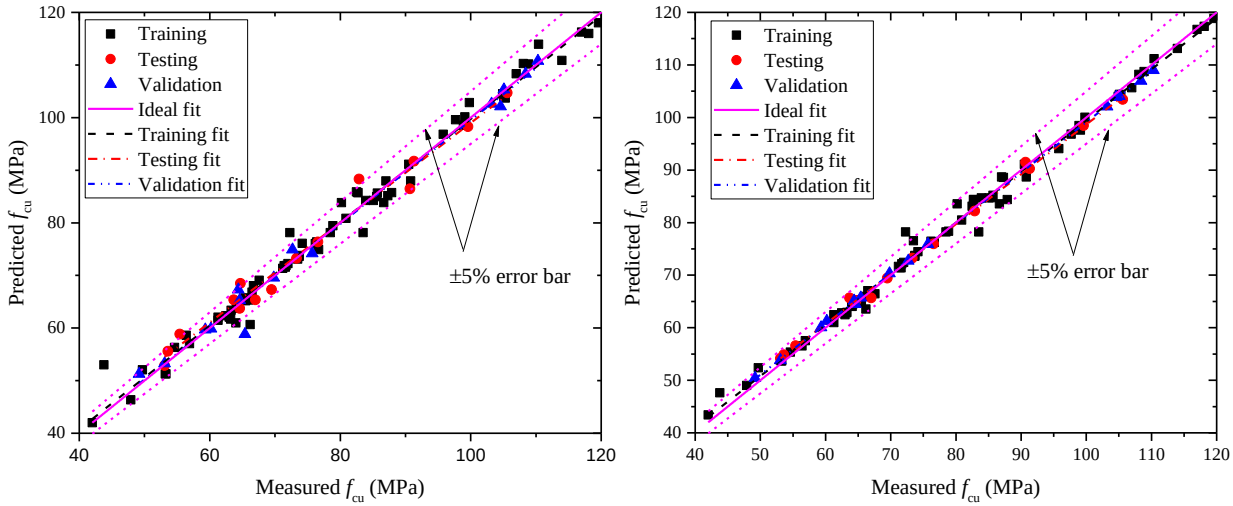

(a) ANN (b) GPR

Fig. 8. Comparison of the measured ultimate strength with the predicted values

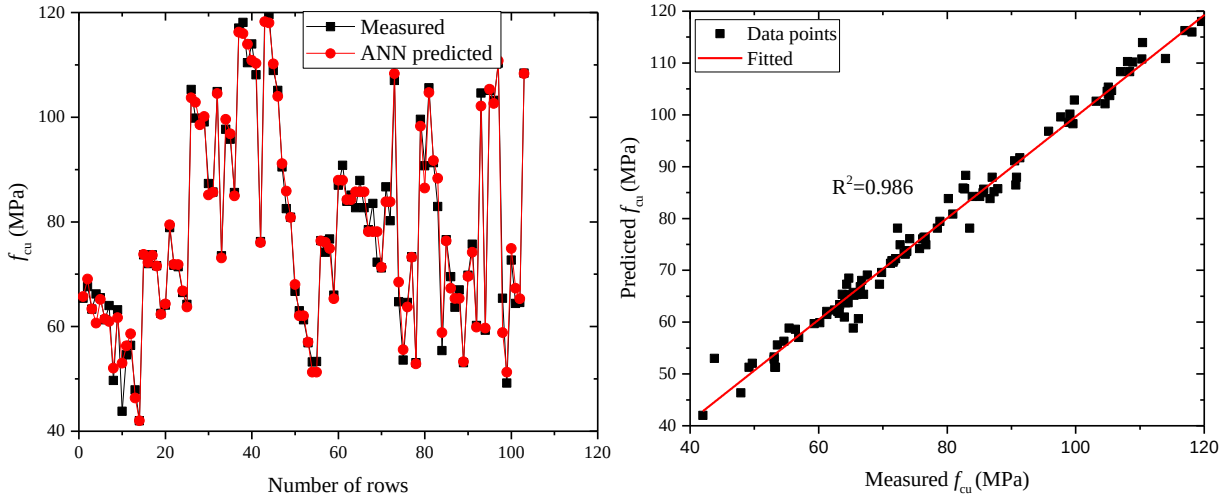

(a) ANN prediction (b) Coefficient of determination

Fig. 9. Performance of the developed ANN model

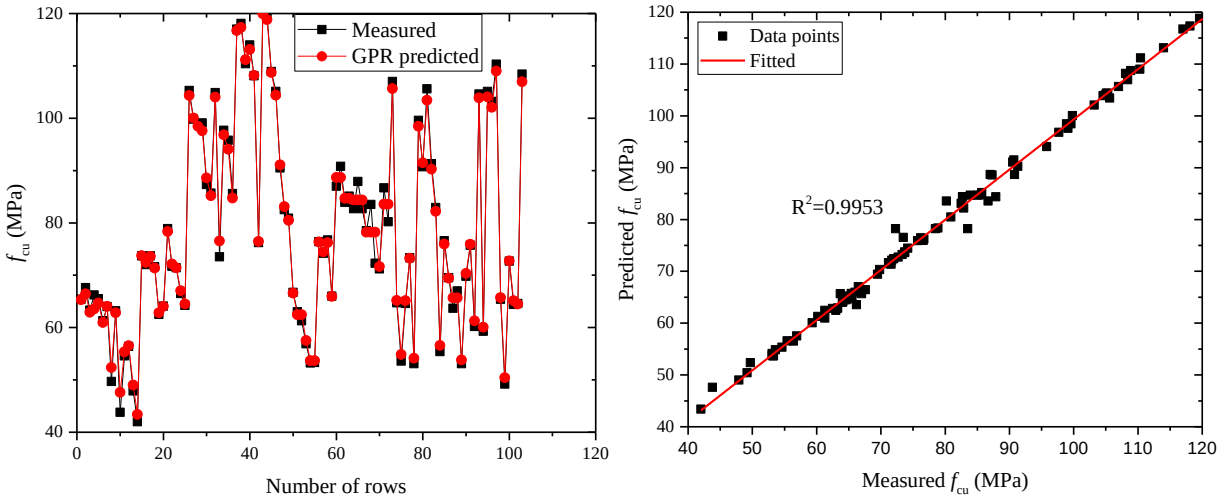

(a) GPR prediction (b) Coefficient of determination

Fig. 8. Performance of the developed GPR model

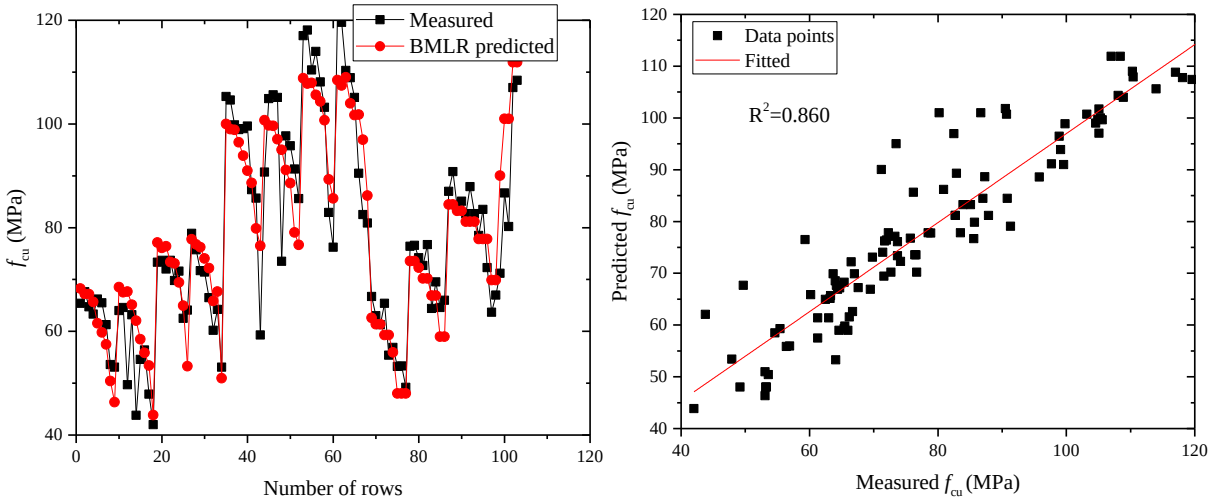

(a) BMLR prediction (b) Coefficient of determination

Fig. 9. Performance of the developed BMLR model

Table 1. Test database used in the model

Reference	ρ	f_{co} (MPa)	δ (%)	E_f (GPa)	t_f (mm)	ε_f (%)	f_{cu} (MPa)
Wu et al. [18]	1.0	31.7	0	235	0.167	1.76	65.4
		31.7	2.5				67.6
		31.9	2.9				64.7
		32.4	7.2				63.3
		30.9	14.9				66.2
		32.6	21.6				65.5
		32.6	27.2				61.3
		32.6	44.1				53.6

		34.3	56.3			53.1
		32.1	0			64
		32.1	2.3			64.6
		32.7	2.9			49.7
		32.4	8.5			63.2
		31.3	14.3			43.8
		29.3	20			54.6
		31.5	29.5			56.4
		31.6	35.5			47.9
		30	56.1			42
		46.4	0			73.3
		46.4	2.5			73.7
		47.2	2.9			72
		44.6	6.4			73.7
		47.3	11			69.8
		42.3	12.5			71.6
		45.5	27.9			62.5
		45.7	56.2			64.1
		47.4	0			78.9
		47.4	2.3			75.7
		46.9	2.9			71.7
		47.3	8.7			71.4
		48	14.2			66.5
		42.8	21.9			60.2
		46.6	23			64.2
		43.1	58			53.1
		33.3	0			105.3
		33.3	2.4			104.6
		33.4	2.9			99.8
		32.9	7.9			98.9
		33.5	15			99.1
		33.1	21.3			99.6
		33	26.9	0.334		87.3
		29.6	43			85.7
		33.7	57			59.3
		34.5	0			90.7
		34.5	2.4			104.9
		34.7	2.9			105.6
		34	8.1			105.1

		35	14.4				73.5
		32.5	20.2				97.7
		32.8	26.7				95.8
		32.1	48.5				91.3
		33.5	56.2				85.6
		47.9	0				117
		47.9	2.5				118.1
		48.4	2.9				110.4
		47.9	7.7				114
		47.1	9.6				108.1
		49.1	21.2				103.2
		49.1	48.5				82.9
		48.3	56.2				76.2
		47.3	0				121.1
		47.3	2.5				119.6
		50.2	2.9				110.3
		45.7	8.4				108.9
		46.1	14.4				105.1
		49	18.4				90.5
		46.9	27				82.5
		47	53				80.9
Li et al. [11]	0.2	43.8	0	258	0.334	1.49	66.7
		43.8	3				63
		43.8	3				61.3
		43.8	8				65.4
		43.8	8				55.4
		43.8	16				56.9
		43.8	35				53.2
		43.8	35				53.3
		43.8	35				49.2
	0.4	43.8	0				76.4
		43.8	0				76.6
		43.8	3				74.2
		43.8	8				72.7
		43.8	8				76.7
		43.8	16				64.4
		43.8	16				69.5
		43.8	35				64.6
		43.8	35				66

	0.6	43.8	0				87
		43.8	0				90.8
		43.8	3				83.9
		43.8	3				85.1
		43.8	8				82.7
		43.8	8				87.9
		43.8	8				82.7
		43.8	16				78.5
		43.8	16				83.5
		43.8	16				72.3
		43.8	35				63.7
		43.8	35				67
	0.2	43.8	8		0.501		71.2
	0.4	43.8	8				86.7
		43.8	8				80.2
	0.6	43.8	8				107
		43.8	8				108.4
Minimum	0.2	29.3	0	235	0.167	1.49	42
Maximum	1.0	50.2	58	258	0.501	1.76	121.1

Table 2: Model summary

Number of data	Multiple R	R-Square	Adj R-square	Root-MSE (SD)	Rows missed
103	0.92733	0.85995	0.85423	7.37383	0

Table 3: ANOVA

	DF	Sum of Squares	Mean Square	F Value	Prob>F
Model	4	32718.67	8179.667	150.435	0
Error	98	5328.594	54.37341		
Total	102	38047.26			

Table 4: Model coefficients

	Value	Standard Error	t-Value	Prob>|t|
Intercept	-36.3138	6.94614	-5.22791	9.70E-07
$2r/b$	54.66411	3.01586	18.12556	0
f_{co} (MPa)	0.60366	0.12343	4.89053	3.94E-06
δ(%)	-0.41691	0.04405	-9.46516	1.78E-15
t_f	184.2782	9.38386	19.63779	0

Table 5. Weights and biases of the selected 4-15-1 architecture

Hidden layer	w_1				w_2		
	2r/b	f_{co}	δ	t_f	f_{cu}	b_1	b_2
1	-0.01938	-7.50709	-4.6926	3.995774	2.282845	-5.02756	
2	1.106473	-4.15193	-5.05247	0.341523	1.377044	-4.33042	
3	-1.0399	1.528196	2.524318	-1.45428	5.920234	2.625794	
4	2.560789	3.717715	-2.5806	-1.68423	-3.92895	-2.97694	
5	0.797232	3.538876	-1.87743	1.609724	6.256812	-3.15424	
6	-3.18243	-7.76703	5.295658	2.174151	-2.22012	3.20949	
7	2.059885	-2.49536	5.352248	4.529893	-1.73519	3.662914	
8	-0.11631	6.532017	-4.04565	5.193886	-1.77226	-2.56795	-3.78534
9	3.519138	1.864404	5.024643	-3.54999	-2.56933	-0.07049	
10	2.074723	-2.45226	-4.53085	-0.03322	-1.45121	-0.28007	
11	-1.89158	1.820149	2.649225	-1.16391	3.941276	-1.69566	
12	3.45564	5.516056	-1.18055	1.317115	3.833241	3.23313	
13	2.012213	-3.71056	1.279575	0.13646	3.588699	1.425177	
14	-2.19674	1.453738	7.478569	-0.33409	-4.00513	-4.39537	
15	2.850122	-1.91109	-1.04956	-2.88285	2.442951	0.862346	

Table 6. Performance of different GPR architecture

Covariance function	Performance	Training	Testing	Validation
LINiso	R^2	0.8106	0.0923	0.9134
	MSE	79.01401	484.2778	31.12219
LINard	R^2	0.8106	0.8841	0.9134
	MSE	79.01406	32.20567	31.12219
SEard	R^2	0.978	0.9986	1
	MSE	8.157397	0.363	1.04E-10
RQiso	R^2	0.9335	0.9588	0.9868
	MSE	24.74966	11.59434	6.595863
Qard	R^2	0.9388	0.9634	0.9921
	MSE	22.84994	10.28349	4.917461
Materniso ½	R^2	0.9939	0.9976	0.9999
	MSE	2.420955	1.249059	0.744415

Table 7. The statistical evaluation of the proposed models

	ANN		GPR	
	R^2	MSE	R^2	MSE
Training	0.9866	4.9894	0.9939	2.4210
Testing	0.9778	6.0552	0.9976	1.2491
Validation	0.9896	4.7290	0.9999	0.7444

Table 8. Statistical evaluations of the models (whole datasets)

Models	MSE	R^2
ANN	5.1067	0.9862
GPR	2.0061	0.9953
BMLR	51.7339	0.8599

A brief technical biography

I.A Tijani received his B.Tech from Ladoke Akintola University of Technology, Nigeria; MSc from King Saud University, Saudi Arabia; and PhD from the City University of Hong Kong. His research interests include the constitutive modeling of concrete, strengthening and repairing of concrete, and infrastructural management.

A.I Lawal received his B. Eng and M. Eng degrees from the Federal University of Technology, Akure Nigeria and PhD from the City University of Hong Kong. Currently, he is a Senior Lecturer in the Department of Mining Engineering at Federal University of Technology, Akure. His research interests include the sustainable mining engineering, rock mechanics, geotechnics and artificial intelligence applications.

Nafiu Olanrewaju Ogunsola received his B. Eng and M. Eng degrees in the Department of Mining Engineering from the Federal University of Technology Akure, Nigeria, in 2012 and 2016, respectively, and is currently a final-year Ph.D. candidate in the Department of Mineral Resources and Energy at Jeonbuk National University, South Korea. Prior to starting his doctoral study in 2019, he worked with mining companies in Nigeria, including the China Civil Engineering Construction Corporation (CCECC) and Dangote mines. His current research interests include rock mechanics, rock dynamics, rock fracture mechanics, blasting technology, and the application of machine learning to rock mechanics.

Sangki Kwon obtained his BSc and MSc degrees in Department of Mineral Resources and Petroleum Engineering from Seoul National University, Korea, in 1987 and 1989, respectively, and his PhD in Mining Engineering from University of Missouri-Rolla, USA, in 1996. He had worked for Korea Atomic Energy Research Institute (KAERI) from 2000 to 2011. Currently, he is a Professor in the Department of Energy Resources Engineering at Inha University, Incheon, Korea. His research interests are rock mechanics for underground excavation, thermo-hydro-mechanical (THM) coupling analysis for high-level radioactive waste disposal, analysis of time-dependent deformation of rock, characterization of excavation damaged zone around an underground opening, investigation of blasting impact, and application of artificial neural network in rock mechanics.